Chapter 6

THE INTERACTION SURFACE BETWEEN Zα AND Z-DNA

Mapping of the Zα/Z-DNA interaction surface in solution

In order to map the interaction surface between Zα and Z-DNA in solution, we have recorded 2D ^{15}N-HSQC NMR spectra of free and bound Zα. Using this technique, chemical shift changes in backbone and side chain amides are detected when DNA is bound in the vicinity [207]. The superposition of the ^{15}N-HSQC spectra of free Zα and $(Z\alpha)_2$/Z-DNA complex shows that several amide resonances move significantly, a few vanish and many show insignificant effects as a result of Z-DNA binding (fig. 48). We considered chemical shift changes with $(\Delta^1H + \Delta^{15}N/10) > 0.1$ ppm or vanishing cross peaks indicative of closeness to the bound Z-DNA (labeled in capital letters in fig. 48). Most significant chemical shift changes map to α3 (red in fig. 50), which has the characteristics of a recognition helix as shown by mutagenesis [5]. Further chemical shift changes are observed at the N-terminus of α2 and around W195. The shift changes of G151 and G163 may reflect a slight long-range conformational change resulting from Z-DNA binding. Such effects have been observed for glycines occupying hinge positions in the protein backbone [207]. The quality of the chemical shift data is underlined by the good superposition of the N-terminal residues 118 – 123 (labeled in *italics* in fig. 48), which are outside the core domain and do not contact the Z-DNA.

Investigation of the „folded" peaks of imino groups of arginine side chains shows that only R174 shifts upon Z-DNA binding, whereas the other two arginine imino groups present in Zα remain unaffected (lower right box in fig. 48). In addition, the well resolved aromatic side chains of the two tyrosines in Zα could be mapped by 1D ^{1}H NMR in D_2O (fig. 49). Both the Hδ and Hε resonances of Y177 vanish when Zα is titrated with substrate DNA, while those of Y136 remain unaffected. Taken together, chemical shift changes in four side chains (highlighted in fig. 50) and 13 backbone amides (red in fig. 50) were found by interaction mapping suggesting that Zα binds Z-DNA mainly through α3 and through additional interactions in the vicinity of W195 and the N-terminus of α2.

fig. 48 **Interaction mapping by ^{15}N-HSQC NMR spectroscopy (see next page).** The superposition of the ^{15}N-HSQC spectra of free Zα (black) and of bound Zα (red) identifies residues (labeled with capital letters) whose amide chemical shift changes substantially upon binding Z-DNA, indicating that they are in the vicinity of the Z-DNA ligand. Reference residues at the unstructured N-terminus are unaffected (labeled with small letters).

fig. 49 **Mapping of aromatic side chains by 1D ^{1}H NMR spectroscopy in D_2O (see page after next).** The aromatic atoms Hδ and Hε of Y177, but not Y136, vanish when Zα is titrated with substrate DNA. This indicates that the aromatic ring of Y177, but not Y136, is in the vicinity of bound Z-DNA.

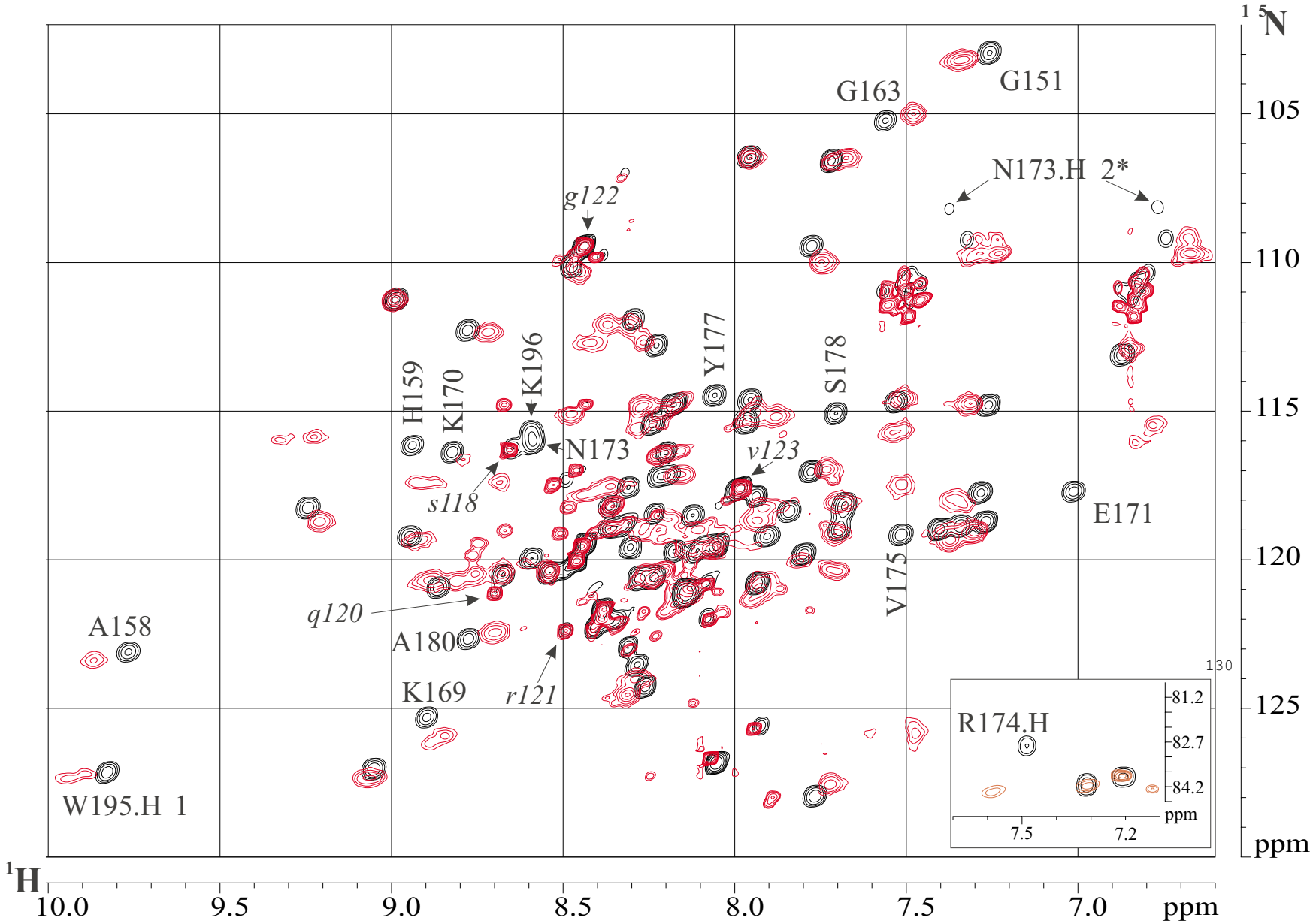
15N
105
110
115
120
125
130
ppm
G163
G151
N173.H 2*
g122
H159
K170
K196
Y177
S178
N173
v123
s118
E171
V175
q120
A158
A180
K169
r121
W195.H 1
R174.H
81.2
82.7
84.2
ppm
7.5
7.2
1H
10.0
9.5
9.0
8.5
8.0
7.5
7.0
ppm

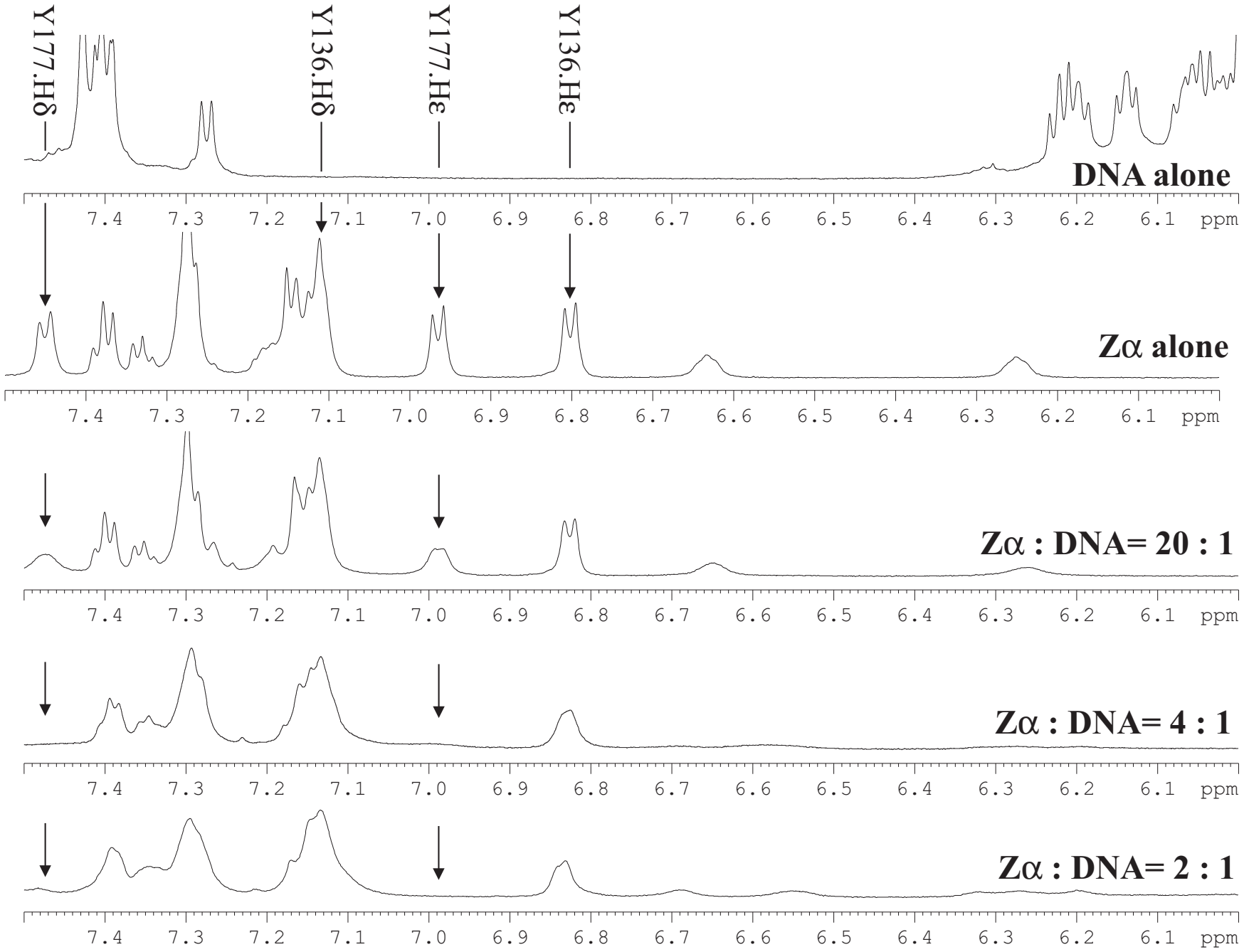
Y177.Hδ
Y136.Hδ
Y177.Hε
Y136.Hε
DNA alone
Zα alone
Zα : DNA= 20 : 1
Zα : DNA= 4 : 1
Zα : DNA= 2 : 1
7.4 7.3 7.2 7.1 7.0 6.9 6.8 6.7 6.6 6.5 6.4 6.3 6.2 6.1 ppm

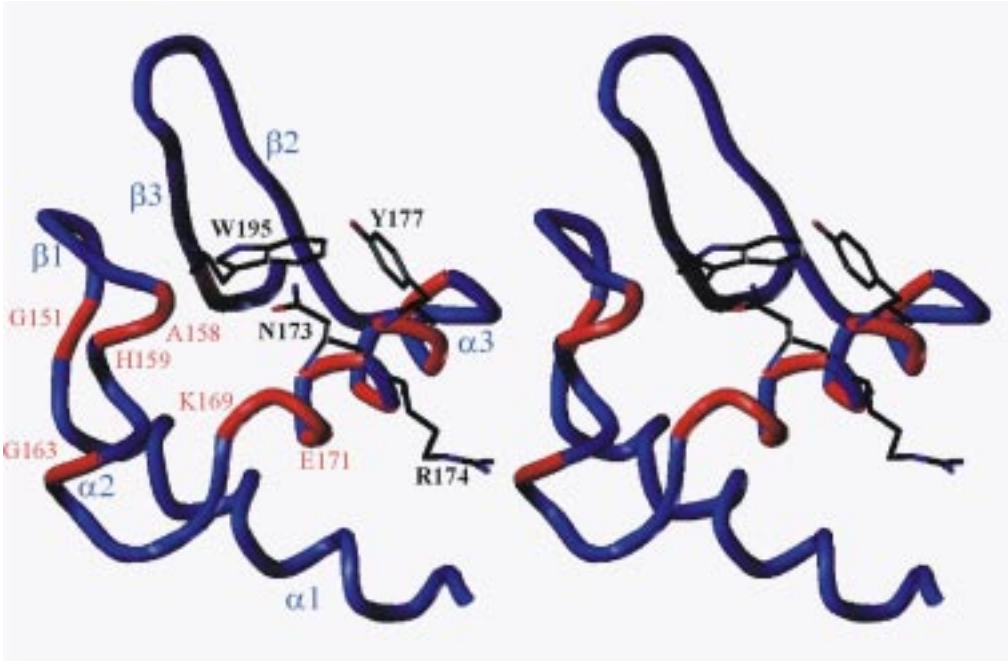

fig. 50 **Interaction map of the Zα/Z-DNA complex**. The stereo view of residues with NH chemical shift changes in the backbone (red tube) and in the side chain (highlighted) shows that they form a contiguous interaction surface on α3 and part of the β2β3-sheet of Zα, except for the two glycines G151 and G163.

Electrostatic potential surface of Zα

Protein/DNA interactions are characterized by a large number of salt bridges and hydrogen bonds, as a recent analysis of 26 high resolution protein/DNA complexes has shown [49]. The Zα domain (residues 119-200) possesses a net positive charge at neutral pH (theoretical pK_a = 8.7) suggesting that interactions between positively charged amino acids and the negatively charged Z-DNA backbone play an important role. The electrostatic surface potential (GRASP [208]) representation of Zα (fig. 51) shows that the four lysines and one arginine on α3 form a highly positively charged surface. The C-terminal β-sheet contributes one positive charge through K187 and a non-charged H-bond donor through the indole ring of W195. Together, α3 and the β-sheet have the shape of a half-opened left hand (see fig. 50). The positive pole of the net electric dipole moment of Zα (pink arrow head in fig. 51) points out of this hand, indicating that this is the most favored point of contact for the negatively charged DNA.

In order to demonstrate that the electrostatic potential surfaces of Zα and Z-DNA are complementary, we schematically docked the Zα domain to the Z-DNA hairpin $d(CG)_3T_4(CG)_3$ that was investigated by the aforementioned binding and interaction mapping studies. The Z-DNA hairpin, whose crystal structure is known [171], has two Zα binding sites

with similar binding constants [4] suggesting that both binding sites are similar. Of the residues identified by interaction mapping, six positively charged or potentially H-bonding residues, K169, K170, N173, R174, Y177 and W195, belong to the contiguous surface of the half-opened hand. By using scanning mutagenesis, residues K169, N173, Y177, K181 and W195, were shown to diminish Z-DNA affinity when mutated to alanine. The side chain H-bond donors of these residues (labeled in fig. 51) were used as candidate Z-DNA contacts to guide the docking attempt. The Zα domain and the Z-DNA hairpin were arranged so that each of the candidate Z-DNA contacts has a minimal distance to a suitable H-bond acceptor on the negatively charged Z-DNA backbone. The electrostatic surface representation of the schematically modeled $(Z\alpha)_2$/Z-DNA complex shows that the half-opened hand is suitably shaped to sit on the phosphate backbone strand of Z-DNA where it forms favorable ionic and H-bond interactions (fig. 51). For clarity, the Zα domain is shown at a distance of approximately 6 Å between the Zα side chains and the Z-DNA backbone. The second Zα domain in this scheme binds in an identical manner to the opposite phosphate backbone strand of the Z-DNA hairpin.

The model illustrates that the interaction surface of Zα is of suitable size to cover 6 basepairs of Z-DNA consistent with the biochemical binding data shown in this work. Furthermore, this low resolution model derived from interaction mapping and mutagenesis data in solution, is consistent with the high resolution crystal structure of Zα complexed with Z-DNA [6] showing a two-fold symmetry between both bound Zα domains. In the crystal structure Zα contacts exclusively the phosphate backbone of Z-DNA, except for one van der Waals contact to a guanine base, suggesting that the distinct backbone of Z-DNA is primarily responsible for specific recognition by Zα. In conclusion, these data show that Zα is well shaped and equipped with positive charges to specifically bind to 6 basepairs of Z-DNA as a pair from opposite sides.

Comparison of the solution structure of free Zα with the crystal structure of Zα complexed with Z-DNA

The superposition of the ensemble of 15 solution structures of free Zα with the crystal structure of the $(Z\alpha)_2$/Z-DNA complex [6] shows that the structures of free and bound Zα are almost identical (fig. 43). The backbone rmsd is 0.75 Å (residues Y136-E148 and A155-A198), and the non-hydrogen atom rmsd of buried residues (highlighted in fig. 47) is 1 Å,

fig. 51 **Electrostatic potential surface representation of two Zα domains docking to the Z-DNA hairpin $d(CG)_3T_4(CG)_3$ (see next page).** Positive, negative and neutral electrostatic potentials are colored blue, red and white, respectively. The Zα domain on the left is oriented so that helix α3 points into the plane of the figure and that the loop between β2 and β3 is exposed in the upper right part of the domain. Helix α1 resides on the back left with its N-terminus labeled (N). The deep and narrow minor groove of the Z-DNA hairpin, which is flanked by negatively charged phosphodiester moieties, faces the observer. The uncharged top (white) of the Z-DNA hairpin represents the T_4 loop, where hydrophobic thymine bases are exposed. The positively charged residues of α3 and the C-terminal β-sheet form a contiguous surface with the shape of a half-opened left hand from where the positive pole of the net electric dipole moment (pink arrow head) projects. Zα is suitably shaped and charged to bind to the phosphate backbone of 6 basepairs of Z-DNA.

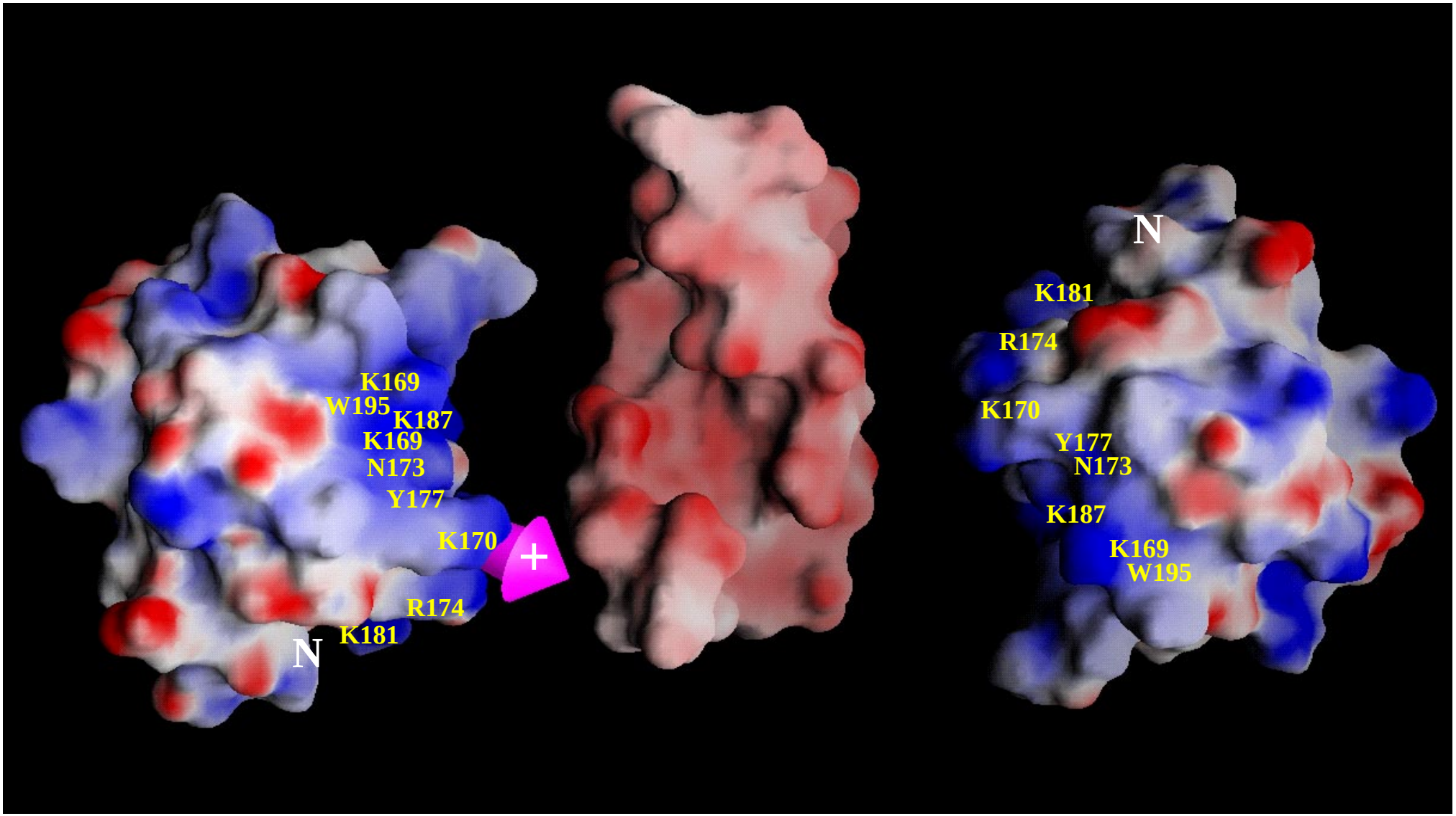
K169
W195
K187
K169
N173
Y177
K170
R174
K181
N
+
N
K181
R174
K170
Y177
N173
K187
K169
W195

underscoring the high similarity of the solution and crystal structures of Zα. Even the flexibility of the α1β1-loop (residues G151-G153) is reflected by the high B-factors in the crystal. The NMR structure was determined independently from the crystal structure. Small local differences in the backbone of Zα (rmsd 1 – 2 Å) are observed between G163 and L165 suggesting that the chemical shift change of G163 reflects a minor rearrangement in the C-terminus of α2 when Zα binds Z-DNA. However, overall Zα does not undergo any significant conformational changes upon binding Z-DNA.

The interaction surface between Zα and Z-DNA of the crystal structure also agrees well with that mapped in solution (fig. 50 and fig. 52). N173, R174, Y177 and W195, which show significant side chain chemical shift alterations, also mediate Z-DNA contacts in the crystal structure. The vicinity of the Z-DNA is also sensed by several backbone amides in α3 and those of A158 and H159 in α2. The NH of A158 coordinates a well-defined water with the NHε of W195, and the amide of H159 mediates a phosphate backbone contact relayed by two waters in the crystal structure. The chemical shift changes in these two residues suggest that these waters may be rearranged upon Z-DNA binding. The roles of P192 and P193, which contact Z-DNA in the crystal structure, could not be determined because prolines are insensitive to the ^{15}N-HSQC mapping technique. Overall, the interaction map revealed changes in the medium-range environment of Zα as a result of contact with Z-DNA. These changes in the backbone amides of α3 and α2 complement the short-range information gained from the Zα/Z-DNA contacts in the crystal structure.

Of the nine Z-DNA residues contacting DNA observed in the crystal structure, the side chains of K169, N173, Y177 are partially ordered and those of T191, P192, P193, W195 are well ordered in the solution structure of free Zα (fig. 52). Only two Z-DNA contacts, K170 and R174, are flexible. NOEs between the methyl group of T191 and P192 (fig. 40 and fig. 46) lock the T191 side chain in the same orientation as in the crystal structure, even though T191 is totally exposed in free Zα. In the majority of our solution-state structures, NOEs to the δ protons of N173 (fig. 39) hold its amide group in almost the same orientation as that used to mediate a Z-DNA contact in the crystal, suggesting that some of the well-defined waters coordinated by N173 may already be in place in free Zα. Also several NOEs show that the aromatic ring of Y177 is packed against W195 (fig. 41) and N173 in free Zα. In the bound state Y177 maintains these hydrophobic contacts, but is restricted in its rotational freedom as a result of van der Waals contact with a guanosine base of Z-DNA. This establishes a chain of contacts between W195 to Y177 to the guanosine base in which the aromatic rings of each residue lie almost perpendicular to the others and probably relates to the quenching of W195 fluorescence observed when Za binds Z-DNA [169].

Interestingly, the flexibility pattern of the Z-DNA contacting side chains is mirrored by the B-factors of bound Zα in the cocrystal [6]. The side chains of K169, N173, Y177, P192, P193 and W195 have low B-factors, while those of K170 and R174 have high ones. Correspondingly, the Z-DNA phosphates contacted by K170 and R174 show high B-factors, while those contacted by the prepositioned residues show low B-factors. This data indicates that a Z-DNA contact flexible in the unbound state maintains some flexibility in the bound state. By alanine scanning mutagenesis it was demonstrated that the flexible Z-DNA contacts had nearly no effect on Z-DNA affinity, whereas the partially ordered Z-DNA contacts K169, N173 and Y177 diminished the binding constant 37-, 168- and 26-fold, respectively without affecting the overall stability of the protein [5]. These data suggest that the contribution of a

side chain to binding can be correlated with its relative rigidity in the free and bound state. In the case of K170 and R174, the binding enthalpy gained from forming a hydrogen-bond may be roughly balanced by the loss in binding entropy required to partially order a flexible side chain. In contrast, the unexpectedly rigid residues T191, P192 and P193, forming van der Waals contacts with the Z-DNA, may make a significant contribution to the free energy of binding, consistent with the high conservation and uniqueness of these prolines to the Zα/Zβ family. In conclusion, of a total of nine Z-DNA contacts, seven are already prepositioned in free Zα, indicating that Zα is preshaped to fit Z-DNA.

Prepositioned residues within the DNA binding site are not the rule in all HTH domains. A molecular dynamics simulation of the *Antennapedia* HTH-domain/DNA complex suggests that key DNA contacting side chains, such as Q50, are flexible in the bound state [209]. Also, in the crystal structure of the related *even-skipped* homeodomain/DNA complex, the side chain of the key DNA contacting residue Q50 adopts three different conformations resulting in flexible DNA recognition [33]. The Q50A mutation reduced the DNA affinity only 2.4-fold [210] consistent with our finding that flexible DNA contacts in Zα make minor contributions to the free energy of binding. It is possible that Zα compensates for its significantly smaller interaction surface as compared to other B-DNA binding proteins [6,49] by utilizing rigid prepositioned Z-DNA contacts.

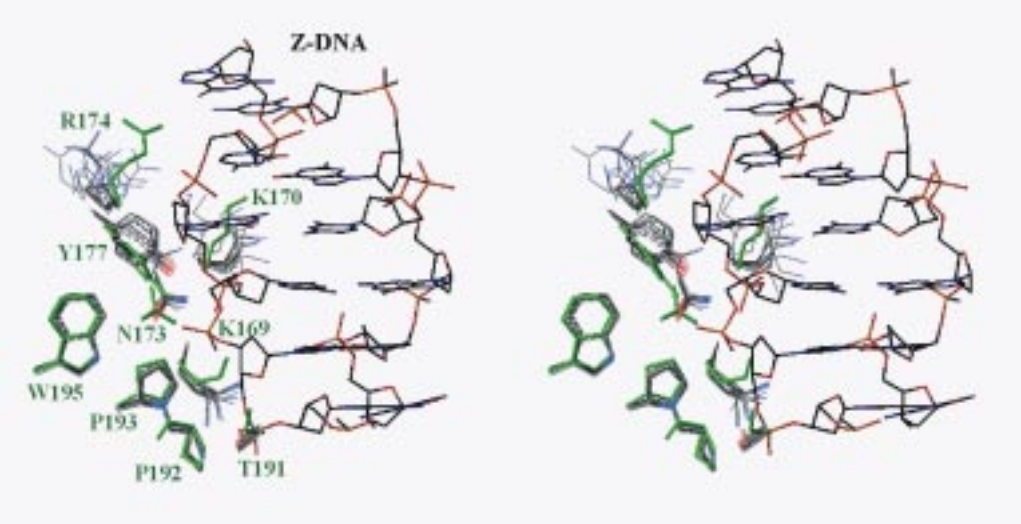

fig. 52 **Zα has a preposition binding surface for Z-DNA.** The superposition of the nine Z-DNA contacting residues (green) of Zα complexed with Z-DNA in the cocrystal with those of the 15 lowest energy NMR structures of free Zα shows that seven of these residues are already prepositioned in free Zα to fit Z-DNA. Only two, K170 and R174, are flexible in solution. Y177 shows rotations around χ2 but not χ1. The structures were superimposed as shown in fig. 43.

Summary

Interaction mapping by ^{15}N-HSQC NMR spectroscopy identified four side chains and 13 backbone amides of Zα that are close to bound Z-DNA. With the exception of G151, G163 and K196, these residues form a contiguous interaction surface on Zα that agrees well with that previously identified by alanine scanning mutagenesis. The electrostatic potential surface of Zα shows that this candidate interaction surface is highly positively charged harboring the positive pole of the overall electric dipole moment. This surface is complementary in both charge and shape to the negatively charged backbone of Z-DNA. This finding is consistent with the high resolution crystal structure of the $(Z\alpha)_2$/Z-DNA complex [6].

Comparison of the solution structure of free Zα with the crystal structure of Zα complexed with Z-DNA [6] demonstrates that seven from a total of nine Z-DNA contacting residues are well ordered and adopt almost identical side chain conformations in free and bound Zα. Five of these seven rigid residues showed a large contribution to the free energy of binding when mutated to alanine, whereas the two flexible Z-DNA contacting residues showed no contribution. This suggests that Zα uses prepositioned residues in order to minimize the entropic cost of binding Z-DNA.